Study of the Chemical Ionization of Organophosphate Esters in Air Using Selected Ion Flow Tube–Mass Spectrometry for Direct Analysis

Mylène Ghislain, Marine Reyrolle, Jean-Marc Sotiropoulos, Thierry Pigot, Hervé Plaisance, Mickael Le Béchec

Study of the chemical ionization of organophosphate esters in air using selected ion flow tube – mass spectrometry (SIFT-MS) for direct analysis

Running Title : Organophosphate esters detection with SIFT-MS

Mylène Ghislain[1], Marine Reyrolle[1], Jean-Marc Sotiropoulos[1], Thierry Pigot[1], Hervé Plaisance[1], Mickael Le Bechec[1]*

[1] Universite de Pau et des Pays de l'Adour, E2S UPPA, CNRS, IMT Mines Ales, IPREM, 64000 Pau, France

Address reprint requests to Mickael Le Bechec, Universite de Pau et des Pays de l'Adour, E2S UPPA, CNRS, IPREM, Institut des sciences analytiques et de Physicochimie pour l'environnement et les Matériaux, UMR5254, Hélioparc, 2 avenue Président Angot, 64053, PAU cedex 9, France, e-mail: mickael.lebechec@univ-pau.fr, phone +335 594 075 84

ABSTRACT: Organophosphate esters (OPEs) are an emerging environmental concern since they spread persistently across all environmental compartments (air, soil, water, etc.). Measurements of Semivolatile organic compounds (SVOCs) are important but not without challenges due to their physicochemical properties. Selected ion flow tube-mass spectrometry (SIFT-MS) can be relevant for their analysis in air because it is a direct analytical method without separation that requires little preparation and no external calibration. SIFT-MS is based on the chemical reactivity of analytes with reactant ions. For volatile and semivolatile organic compound analysis in the gas phase, knowledge of ion-molecule reactions and kinetic parameters is essential for the utilization of this technology. In the present work, we focused on organophosphate esters, semivolatile compounds that are now ubiquitous in the environment. The ion-molecule reactions of eight precursor ions that are available in SIFT-MS (H_3O^+, NO^+, $O_2^{\bullet+}$, OH^-, $O^{\bullet-}$, $O_2^{\bullet-}$, NO_2^- and NO_3^-) with six organophosphate esters were investigated. The modeling of ion-molecule reaction pathways by calculations supported and complemented the experimental work. Organophosphate esters reacted with six of the eight precursor ions with characteristic reaction mechanisms, such as protonation with hydronium precursor ions and association with NO^+ ions, while nucleophilic substitution occurred with OH^-, $O^{\bullet-}$, and $O_2^{\bullet-}$. No reaction was observed with NO_2^- and NO_3^- ions. This work shows that the direct analysis of semivolatile organic compounds is feasible using SIFT-MS with both positive and negative ionization modes.

INTRODUCTION

Organophosphate esters (OPEs) are phosphoric acid esters with alkyl, chlorinated alkyl or aryl groups instead of a hydrogen at the phosphate group. They are semivolatile organic compounds (SVOCs) that are used in a variety of consumer products. Since brominated flame retardants were phased out, the production of OPEs has increased.[1-3] While OPEs are most commonly used for fireproofing polyurethane foams,[3,4] they have many other applications in a wide variety of everyday consumer products, such as plasticizers and solvents in thermoplastics, electronic devices, oils, lubricants and polishes, food packaging and even baby products.[5-8]

Due to their physicochemical properties, organophosphate esters can diffuse into products and be released into the environment by volatilization, abrasion or leaching.[2,9] These compounds can spread in the environment, and since they are persistent, especially chlorinated OPEs, they accumulate in many environmental media. Numerous studies have shown that OPEs are ubiquitous in indoor environments, such as air (from a few dozen to several hundred ng/m^3), aircraft cabins, dust, and airborne particles,[7,10,11] and outdoor environments, such as air, soil, water, sediments and biota.[12-16] Consequently, living organisms, including humans, are continuously exposed to OPEs. There are multiple human exposure pathways: inhalation,[17,18] ingestion with food and water,[19-21] hand-to-mouth contact[22] and dermal uptake.[18,21,23] The biomonitoring of organophosphate esters and their metabolites in urine, blood, and breast milk has demonstrated these widespread exposure pathways, and some studies have established relationships between OPE concentrations in indoor dust, air and human biological samples.[11,24-27]

In recent years, an increasing number of studies have documented that organophosphate esters may have adverse effects on living organisms, including humans.[28] Correlations have been established between the presence of OPEs in indoor environments and in respiratory allergies; for example, tributyl phosphate (TBP) is significantly associated with the prevalence of allergic rhinitis and asthma.[29] Some organophosphates are known or suspected to be carcinogenic, reprotoxic, neurotoxic or teratogenic.[30,31] Tricresyl phosphate (TCP), especially the ortho isomer, is neurotoxic to humans.[32, 33] OPEs can also interfere with the functions of the endocrine system and induce adverse effects on organisms These endocrine disruptors can alter growth and development or affect the reproductive system and may be involved in the development of hormone-dependent cancers.[2,28,36,37]

Because of their global use and their proven or suspected health effects, organophosphate esters have become compounds of major environmental health concern in recent years. As a result, many methods have been developed recently to measure these compounds. For their analysis in air, passive samplers[38,39] have been used as well as solid phase extraction (SPE) cartridges or membranes[40,41] or solid phase microextraction (SPME)[4,42,43] procedures coupled with gas chromatography – mass spectrometer (GC-MS), GC – atomic emission detection (AED), GC – flame ionization detection (FID), GC – flame photometric detection (FPD) or liquid chromatography – mass spectrometry (LC-MS).[2] The main technical constraint of these analytical methods is the calibration setup, which requires the generation of standard atmospheres. Permeation tubes or syringe-injection methods are not suitable for SVOCs like organophosphate esters because of the very low volatility of these compounds. Furthermore, due to their low vapor pressure, these compounds can be partially sorbed or deposited onto the inner surfaces of the gas-generating devices and pipes, inducing a substantial memory effect.[44]

Selected ion flow tube-mass spectrometry (SIFT-MS) is a well-established direct injection mass spectrometry instrument for the direct and rapid analysis of VOCs in the gas phase up to the parts-per-trillion by volume (pptV) level.[45] This method is currently widely applied in environmental fields because of its high-frequency analysis rate (few minutes per measurement) and ease of use.[46,47] SIFT-MS technology is based on the soft chemical ionization of analytes by reagent ions (H_3O^+, NO^+, $O_2^{\bullet+}$, OH^-, $O^{\bullet-}$, $O_2^{\bullet-}$, NO_2^- and NO_3^-), and the known kinetic parameters of these ion-molecule reactions are used to determine the analyte concentrations.[48] Thus, the main advantage of this technique lies in its potential to achieve quantification without calibration and therefore without the generation of standard atmospheres.

SIFT-MS technology has proven to be relevant for the analysis of SVOCs, such as sesquiterpenes, pesticides and organophosphate compounds,[49-51] but to date, data on the negative ionization mode remain sparse. Understanding the relevant ion-molecule reactions is currently a key objective in SIFT-MS analysis.[52] Knowledge of the product ions formed, together with kinetic data, is essential for the correct quantification of target compounds.

Thus, in the present work, a study of the SIFT-MS reactivity of organophosphate esters with both positive and negative reagent ions was carried out to provide the necessary data for the detection and quantification of these compounds in the gas phase. In addition to SIFT-MS experiments on pure compounds, a computational approach was used to obtain a better understanding of the ion-molecule reactions in the flow tube and for the possible prediction of the reactivity of organophosphate esters. This approach has been shown to be particularly relevant in previous studies.[53-55]

METHODS

Chemicals. Triethyl phosphate (TEP) (99%) was purchased from Merck (Darmstadt, Germany). TBP (≥99%) and tris(2-chloroethyl)-phosphate (TCEP) were purchased from Sigma–Aldrich (St. Louis, MO, USA). Tris-(chloropropyl)-phosphate (TCPP) (98%) and triphenyl phosphate (TPP) (98%) were provided by ICL-products (Terneuzen, The Netherlands). The chlorine-containing compounds (TCEP and TCPP) were both mixtures containing different natural isotopes of chlorine (^{35}Cl and ^{37}Cl). All target compounds are detailed in Table 1.

Selected Ion Flow Tube-Mass Spectrometry (SIFT-MS). Chemical ionization of the organophosphate esters was studied with a Voice 200 Ultra SIFT-MS (SYFT Technologies, Christchurch, New Zealand). This commercial system was equipped with a dual source producing both positive and negative soft-ionizing reagent ions within the same scan. To date, eight precursor ions are available: H_3O^+, NO^+, $O_2^{\bullet+}$, OH^-, $O^{\bullet-}$, $O_2^{\bullet-}$, NO_2^- and NO_3^-. The negative precursor ions, hydroxide ions (OH^-) and superoxide ions ($O_2^{\bullet-}$), were produced from wet air, and the $O^{\bullet-}$, NO_2^- and NO_3^- ions were produced from dry air in a microwave plasma. Each reagent ion was first sequentially selected by a quadrupole mass filter and then injected into the flow tube. The sample was introduced through a heated inlet line (373 K) into the flow tube at a flow rate of 20 ml min^{-1}. The carrier gas was nitrogen (air liquid, Alphagaz 2). The flow tube temperature was maintained at 393 K at a pressure of 0.48 torr. The product ions were analyzed by a second quadrupole in a m/z range from 15 to 400.

For a reaction between a precursor ion R and an analyte A leading to the formation of a product ion P with a reaction rate constant *k*, the quantification with SIFT-MS is based on the following calculation:

$$[A] = \frac{[P] \times ICF_P}{t_r \times k \times [R] \times ICF_R} \quad (1)$$

where ICF_P is the instrument correction factor of the product ion, ICF_R is the instrument correction factor of the precursor ion, and t_r is the reaction time in the flow tube. External calibration is not needed if the value of the reaction rate constant is known. *ICF* factors enable the consideration of the mass discrimination and differential diffusion of each *m/z*. [*P*], [*R*] and t_r are measured parameters.

Gaseous Atmosphere Generation. Gaseous atmospheres of phosphorus flame retardants were generated by spiking 10 µL of pure liquid compounds into a 114 mL microchamber µCTE250 (Markes international, Llantrisant, UK). To vaporize the injected compounds, the microchamber was heated to 250 °C at a flow rate of 50 mL min^{-1} dry nitrogen. SIFT-MS sampling was carried out at the outlet of the microchamber at a flow rate of 20 mL min^{-1}.

Table 1. List of Phosphorus Flame Retardants Used in This Work

		Formula	CAS	MW	Boiling point (°C)	Vapor pressure (Pa) at 25 °C
TEP	Triethyl phosphate	$(C_2H_5O)_3PO$	78-40-0	182	233	$2.20\ 10^{1}$
TBP	Tributyl phosphate	$(CH_3(CH_2)_3O)_3PO$	126-73-8	266	327	$4.65\ 10^{-1}$
TCEP	Tris(2-chloroethyl)-phosphate	$(ClCH_2CH_2O)_3PO$	115-96-8	284-288[a]	352	$5.21\ 10^{-2}$
TCPP	Tris-(monochloropropyl)-phosphate	$(ClC_3H_6O)_3PO$	13674-84-5	326-330[a]	365	$7.52\ 10^{-3}$
TPP	Triphenyl phosphate	$(C_6H_5O)_3PO$	115-86-6	326	441	$6.29\ 10^{-5}$

TCP	Tricresyl phosphate	$(C_7H_7O)_3PO$	78-30-8	368	476	$8.00\ 10^{-5}$

[a] Depending on the proportions of ^{35}Cl and ^{37}Cl in the molecule.

Quality checks were made to ensure that the compound was vaporized without impurities. To do this, the generated atmospheres were sampled at a flow rate of 50 $ml.min^{-1}$ for 15 min in a stainless tube containing 250 mg of Tenax TA supplied by PerkinElmer (Waltham, MA, USA). The Tenax tubes were then thermodesorbed and analyzed by automated thermal desorption (PerkinElmer TurboMatrix 650 ATD) coupled to gas chromatography (PerkinElmer Clarus 680). The gas chromatograph was equipped with an MS detector (PerkinElmer Clarus SQ 8T). The analytical conditions have been reported in a previous study.[43]

Experimental Study of Ion-Molecule Reactions. Each compound was studied individually. Full-scan mass spectra were recorded sequentially for each of the eight precursor ions (H_3O^+, NO^+, $O_2^{\bullet+}$, OH^-, $O^{\bullet-}$, $O_2^{\bullet-}$, NO_2^- and NO_3^-) in a *m/z* range of 15 to 400 with an integration time of 120 s. Before each measurement, blanks were used to measure the background signal from the nitrogen dilution gas. Some traces of water were detected. The contribution of water to the mass spectra is known and documented for each precursor ion[48] so the corresponding signals could be excluded to identify the signals generated exclusively from the reaction between the precursor ion and the studied analyte.

Investigation of Organophosphate Esters Released from Upholstery Foam Samples. Four combustion-modified high-resilience foams were studied. These foams were intended for the manufacturing of upholstery furniture. No information on the composition and fireproofing classification of these materials was provided. The samples were stored individually in aluminum foil at room temperature.

Samples of dimension 5 × 5 × 2 cm were placed in 1-L glass bottles (Duran, Mainz, Germany) filled with zero air (supplied by an F-DGS (Evry, Rance) Air Zero generator). Screw caps with three GL14 ports (Duran) were used to connect the bottles directly to the SIFT-MS instrument via one sample outlet. A Tedlar bag (Zefon International Inc., Ocala, FL, USA) filled with zero air was connected to the second bottle inlet to compensate for the pressure loss in the bottle during SIFT-MS sampling. The third GL14 port was plugged with a septum. The samples were incubated in closed bottles for 24 h at 23 ± 2°C or at 100 ± 2°C before being connected to the Tedlar bag and to the instrument for a full-scan SIFT-MS analysis.

Computational Details. The molecular geometries and reaction energies were obtained by MP2 optimization using DFT (M062X) and the triple zeta basis set 6-311++g(d,p). All calculations were carried out using a Gaussian16 program.[56] Geometry optimizations were conducted without any symmetry restrictions in the gas phase.

As controlled atmospheres of the organophosphate esters are difficult to generate, ion-molecule reaction kinetics were approached in a theoretical manner by calculating the collision rate constants (k_c). The collisional rate constants were calculated from parametrized trajectory calculations using the polarizability α and the dipole moment μ_D of the neutral (i.e., the studied) molecule derived from DFT calculations and the reduced mass of the ion-molecule complex according to a method described by Su and Chesnavich.[57] For all exothermic H_3O^+ proton transfer reactions, the reaction rate constant k was assumed to be equal to the collision rate constant k_c.[58]

RESULTS AND DISCUSSION

Ion-Molecule Reactions. For positive ionization, data on the ion formation and reaction rate constants are available for TBP in the LabSyft software database, but no article citation is provided, and to our knowledge, there are no published data to date. Our experimental data are in good agreement with those provided by the software but also provide additional information. To date, there are no data in the literature on the gas phase chemical ionization of the other compounds studied in our work.

In this study, ion-molecule reactions were studied for 2 alkylphosphate esters, 2 chlorinated alkylphosphate esters and 2 arylphosphate esters (see Table 1).

The distinctiveness of chlorinated alkylphosphate esters lies in the presence of chlorine atoms at the end of the carbon chains. Due to the natural presence of different chlorine isotopes ($^{35}Cl/^{37}Cl \approx 75/25$), these compounds have highly characteristic mass spectra: the same fragmentation leads to the formation of several product ions whose *m/z* depends on the proportions of the ^{35}Cl and ^{37}Cl isotopes. This observation is known in electron impact mass spectrometry, and it also applies to chemical ionization analyses such as SIFT-MS. Figure 1 illustrates this property of the chlorinated alkylphosphate esters.

Alkylphosphate Esters (Chlorinated and Nonchlorinated). Table 2 summarizes the product ions resulting from the reaction of nonchlorinated (TEP and TBP) and chlorinated alkylphosphate esters (TCEP and TCPP) with the SIFT-MS precursor ions.

H_3O^+ Reactions. A reaction with H_3O^+ leads to the protonation of TEP, TBP and TCEP, forming product ions at *m/z* = 183, 267 and 285(287/289), respectively, according to the following reaction:

$$(RO)_3PO + H_3O^+ \rightarrow (RO)_3POH^+ + H_2O \qquad (2)$$

The protonated compounds are at minima on the potential energy surfaces, and from a thermodynamic point of view, all these reactions are highly favorable (from -37 kcal mol^{-1} for

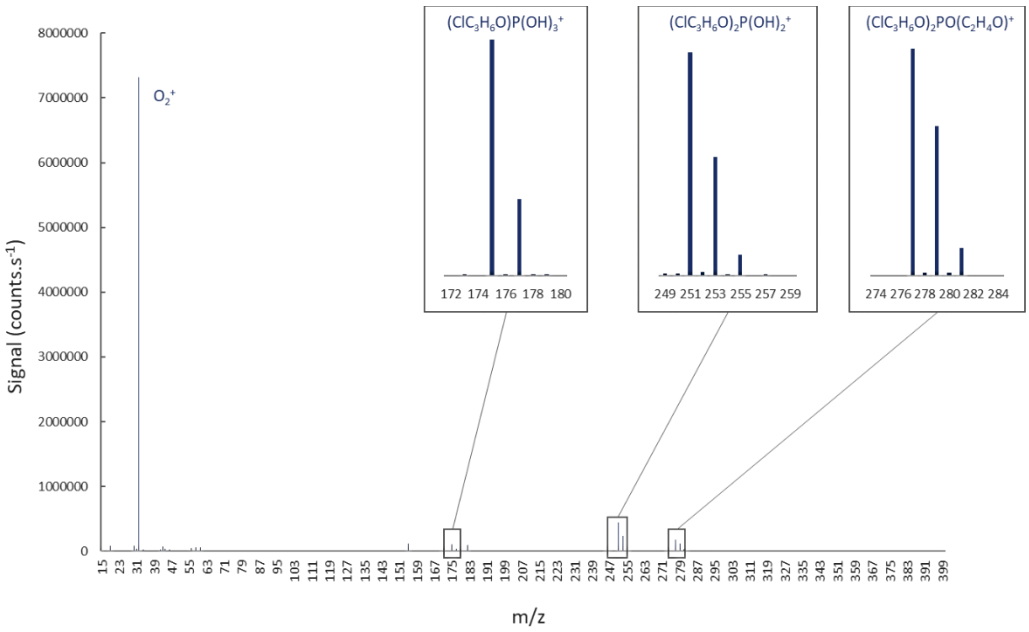

Figure 1. SIFT-MS full scan (m/z range from 15 to 400) of tris-(monochloropropyl)-phosphate with the O_2^+ precursor ion. Flow tube temperature: 393 K, flow tube pressure: 0.48 torr.

Table 2. The Experimental Product Ions and the Corresponding Branching Ratios for the Reactions of Alkylphosphate Esters with Positive and Negative SIFT-MS Precursor Ions in N_2 Gas

Precursor ion	Triethylphosphate MW=182		Tributylphosphate MW=266		Tris(2-chloroethyl)phosphate MW=284-288[a]		Tris-(monochloropropyl)-phosphate MW=326-330[a]	
	Product ions (*m/z*)	BR[b]	Product ions (*m/z*)	BR[b]	Product ions (*m/z*)	BR[b]	Product ions (*m/z*)	BR[b]
H_3O^+	$(C_2H_5O)_3POH^+$ (183) $(C_2H_5O)_2P(OH)_2^+$ (155) *$C_2H_7O^+$ (47)*	98 2 *secondary*	$(CH_3(CH_2)_3O)_3POH^+$ (267) $(CH_3(CH_2)_3O)_2P(OH)_2^+$ (211) *$C_4H_9^+$ (57)*	90 10 *secondary*	$(ClC_2H_4O)_3POH^+$ (285/287/289)	100	$(ClC_3H_6O)_2P(OH)_2^+$ (251/253/255)	100
NO^+	$(C_2H_5O)_3PO.NO^+$ (212)	100	$(CH_3(CH_2)_3O)_3PO.NO^+$ (296)	100	-	-	-	-
$O_2^{\bullet+}$	$(C_2H_5O)P(OH)_3^+$ (127) $(C_2H_5O)_2P(OH)_2^+$ (155) $(C_2H_5O)_3PO^{\bullet+}$ (182)	2 39 59	$(CH_3(CH_2)_3O)P(OH)_3^+$ (155) $(CH_3(CH_2)_3O)_2P(OH)_2^+$ (211) $(CH_3(CH_2)_3O)_3PO^{\bullet+}$ (266)	44 52 4	$(ClC_2H_4O)_2P(C_2H_4O)^+$ (249/251/253) $(ClC_2H_4O)_2P(OH)_2^+$ (223)	78 22	$(ClC_3H_6O)_2PO(C_2H_4O)^+$ (277/279/281) $(ClC_3H_6O)_2P(OH)_2^+$ (251/253/255) $(ClC_3H_6O)P(OH)_3^+$ (175/177)	40 53 7
OH^-	$(C_2H_5O)_2POO^-$ (153)	100	$(CH_3(CH_2)_3O)_2POO^-$ (209)	100	$(ClC_2H_4O)_2POO^-$ (221/223/225) Cl^- (35/37)	10 90	$(ClC_3H_6O)_2POO^-$ (249/251/253) Cl^- (35/37)	12 88
$O^{\bullet-}$	$(C_2H_5O)_2POO^-$ (153)	100	$(CH_3(CH_2)_3O)_2POO^-$ (209)	100	$(ClC_2H_4O)_2POO^-$ (221/223/225) Cl^- (35/37)	20 80	$(ClC_3H_6O)_2POO^-$ (249/251/253) Cl^- (35/37)	13 87
$O_2^{\bullet-}$	$(C_2H_5O)_2POO^-$ (153)	100	$(CH_3(CH_2)_3O)_2POO^-$ (209)	100	$(ClC_2H_4O)_2POO^-$ (221/223/225) Cl^- (35/37)	10 90	$(ClC_3H_6O)_2POO^-$ (249/251/253) Cl^- (35/37)	5 95

[a] Depending on the proportions of ^{35}Cl and ^{37}Cl in the molecule.

[b] BR: Branching ratio (%).

TCEP to -53 kcal mol^{-1} for TBP). In this study, this first reaction was not experimentally observed for TCPP.

In addition, other product ions at *m/z* = 155 (TEP), 211 (TBP) and 251 (253/255) (TCPP) were also observed, demonstrating that another reaction pathway exists (Eq 3). This second pathway for the reaction of TBP with H_3O^+ is not documented in the LabSyft software database.

$$(RO)_3PO + H_3O^+ \rightarrow (RO)_2P(OH)_2^+ + ROH \quad (3)$$

The first reaction (Eq 2) was expected because the protonation reaction leading to MH^+ ion formation is the most widely observed mechanism for the reaction of molecules with hydronium ions.[45] In addition, the reaction between the analyte and H_3O^+ can also lead to fragmentation product ions, as described in Eq 3. Fragmentation is also a very common mechanism associated with hydronium precursor ions.

Compared with the protonation reaction (Eq 2), the thermodynamics are slightly less favorable for the second reaction (Eq 3) ($\Delta E \sim 4$ kcal mol^{-1}), but the reaction is still possible. Experimentally, this results in lower branching ratios for this reaction pathway (2% and 10% for TEP and TBP, respectively, see Table 2).

In a secondary reaction, the neutral alcohol molecules ROH from a previous reaction (Eq 3) can react with H_3O^+. Thus, ethanol from the reaction of TEP with H_3O^+ leads to the formation of $C_2H_7O^+$ ions (*m/z* = 47) and butanol from the reaction of TBP with H_3O^+ leads to the formation of $C_4H_9^+$ ions (*m/z* = 57).[59,60] However, the low concentration of alcohol produced during these reactions cannot sufficiently explain the signals at *m/z* = 47 and 57. The loss of TEP and TBP ($(RO)_3POH^+$ from Eq 2) from the nascent protonated molecules could explain the formation of the ions with *m/z* = 47 and 57, respectively.

It is important to note that an ion with *m/z* 57 could also correspond to $H_3O^+(H_2O)_2$, a hydrated hydronium ion with an ^{18}O isotope.[51] In this work, the reactions were studied in dry nitrogen matrices to limit all interfering reactions arising from the presence of water, carbon dioxide and dioxygen in an air matrix. The low signals at *m/z* 37 (H_3O^+. H_2O) and 55 ($H_3O^+(H_2O)_2$) indicate that there was some water present in the system during the acquisition of the organophosphate scans but at a much lower levels than those observed with TEP and TBP.

NO^+ Reactions. The reaction of alkylphosphates with NO^+ precursor ions leads to the formation of $M.NO^+$ ion-molecule complexes at *m/z* = 212 for TEP and *m/z* = 296 for TBP:

$$(RO)_3PO + NO^+ \rightarrow (RO)_3PO.\ NO^+ \quad (4)$$

This reaction mechanism commonly occurs with the NO^+ precursor ion[46] and is exergonic for the nonchlorinated alkylphosphates and for the chlorinated derivatives (~ -47 kcal mol^{-1} and ~ -37 kcal mol$^{-1,}$ respectively). Nevertheless, for the chlorinated alkylphosphate esters, no reaction with the NO^+ precursor ion was experimentally observed.

Formations of MH^+ ions at *m/z* = 183 for TEP and *m/z* = 267 for TBP were also experimentally observed. A NO^+ reaction leading to the formation of MH^+ ions has not been documented and was surprising, especially in the absence of water in the flow tube. However, it is important to note that $NO^+.H_2O$ monohydrate ions are usually present in the flow tube at concentrations that constitute a few percent of the NO^+ precursor concentration, and they can also act as reagent ions. Thus, the following reaction should also be considered:[61]

$$(RO)_3PO + NO^+.\ H_2O \rightarrow (RO)_3POH^+ + HNO_2 \quad (5)$$

$O_2^{\bullet+}$ Reactions. $O_2^{\bullet+}$ is a precursor ion that is usually less frequently used in SIFT-MS than H_3O^+ and NO^+ due to the multiple ion products that generally result from $O_2^{\bullet+}$ molecular reactions, leading to complex spectra.

For alkylphosphates, it is difficult to determine general reaction mechanisms since a wide variety of product ions are experimentally detected (Table 2). Thus, $M^{\bullet+}$ product ions can be formed from the reaction of these compounds with $O_2^{\bullet+}$ precursor ions via a charge transfer process. This reaction mechanism is commonly observed with the $O_2^{\bullet+}$ precursor ion. Thus, ions at *m/z* = 182 and 266 were experimentally observed for TEP and TBP, respectively. The $(C_2H_5O)_3PO^{\bullet+}$ ion was the major product ion formed from the reaction of TEP with the $O_2^{\bullet+}$ precursor ion with a branching ratio of 59%, while $(CH_3(CH_2)_3O)_3PO^{\bullet+}$ was a minor product ion resulting from the reaction between TBP and the $O_2^{\bullet+}$ precursor ion. The charge transfer process was not experimentally observed for the chlorinated organophosphate esters (Figure 1).

Various other reaction mechanisms were noted. Fragmentations leading to the rupture of one or two alkyl chains occurred; thus, $(RO)_2P(OH)_2^+$ and $(RO)P(OH)_3^+$ product ions were sometimes detected. The loss of an alkyl chain was systematically observed for all the studied alkylphosphate esters (Table 2).

The reactivity of $O_2^{\bullet+}$ with the organophosphate esters is usually difficult to generalize, and additional atypical fragmentations can also occur, such as ruptures within the alkyl chains ($(ClC_3H_6O)_2PO(C_2H_4O)^+$, for TCPP) or the loss of a chlorine atom ($(ClC_2H_4O)_2P(C_2H_4O)^+$, for TCEP).

Negative Ionization. During negative ionization, the same reaction mechanism is consistently observed: a reaction between the organophosphate esters and the OH^-, $O^{\bullet-}$ and $O_2^{\bullet-}$ precursor anions systematically leads to the rupture of an alkyl chain as the single reaction pathway:

$$(RO)_3PO + OH^- \rightarrow (RO)_2POO^- + ROH \quad (6)$$

$$(RO)_3PO + O^{\bullet-} \rightarrow (RO)_2POO^- + RO^{\bullet} \quad (7)$$

$$(RO)_3PO + O_2^{\bullet-} \rightarrow (RO)_2POO^- + RO_2^{\bullet} \quad (8)$$

The computational approach shows that reactions involving the hydroxide anion (Eq 6) are largely favored thermodynamically (-62 to -80 kcal mol^{-1}, for the nonchlorinated and chlorinated alkylphosphate esters, as well as arylphosphates). We can also calculate activation barriers for these reactions. For instance, for TBP, a small barrier of 27.5 kcal mol^{-1} was found, showing that the reaction is also kinetically favored.

In the same way, but to a lesser extent, the formation of the $(RO)_2POO^-$ ion with a $RO_2^{\bullet}$ radical in the reaction with $O_2^{\bullet-}$ (Eq 8) is quite possible from an energetic point of view (from -30 to -42 kcal mol^{-1}).

The reaction of $O^{\bullet-}$ with alkylphosphate esters (from -76 to -89 kcal mol^{-1}) and aromatics (around -100 kcal mol^{-1}) is highly favorable thermodynamically. It should be noted that the formation of the $RO^{\bullet}$ radical as the second product of the reaction (Eq 7) is found as a minimum on the potential energy surface only for the aromatic derivatives (triphenyl phosphate TPP and tricresyl phosphate TCP) and is largely stabilized. For the

nonchlorinated and chlorinated alkylphosphate esters, the $RO^{\bullet}$ radical is only a reaction intermediate stabilized by a hydrogen atom from the alkyl chain.

Significant signals were also noted at *m/z* = 35 and 37 for the chlorinated organophosphate esters, which correspond to the Cl^- chloride ions (isotopes Cl_{35} and Cl_{37}). In this case, an S_N2 nucleophilic substitution reaction should be considered. This substitution leads to the formation of chloride ions and neutral molecules (or radicals) according to the following reactions:

$$(ClRO)_3PO + OH^- \rightarrow (ClRO)_2PO(OROH) + Cl^- \quad (9)$$

$$(ClRO)_3PO + O^{\bullet -} \rightarrow (ClRO)_2PO(ORO^{\bullet}) + Cl^- \quad (10)$$

$$(ClRO)_3PO + O_2^{\bullet -} \rightarrow (ClRO)_2P(ORO_2^{\bullet}) + Cl^- \quad (11)$$

This reaction is made possible by the presence of chlorine atoms, giving the molecule a nucleophilic character. OH^-, $O^{\bullet -}$ and $O_2^{\bullet -}$ ions are known to be good nucleophiles in the gas phase. In this reaction, the product ions are chloride ions, and the neutral molecules and radicals cannot be detected by SIFT-MS. This reaction pathway is highly favorable with high experimental branching ratios (from 80 to 95%).

No reactions were observed between the organophosphate esters and the NO_2^- and NO_3^- precursor ions.

Arylphosphate Esters. Due to the physicochemical properties of the arylphosphate esters such as TPP and TCP, the generation of gaseous atmospheres is complicated; increasing the temperature to 250°C is not sufficient for vaporizing these high-purity semivolatile compounds. The reactivity of these two compounds could not be studied experimentally. However, our experimental work on the alkylphosphate esters (chlorinated and nonchlorinated) highlighted typical reaction patterns, with the exception of the reactions with the $O_2^{\bullet +}$ precursor ion. The energy calculations showed that these different reactions are thermodynamically favorable, including the reactions for the aromatics (TPP and TCP).

Based on these observations, a list of probable product ions from the reactions of TPP and TCP with the various SIFT-MS precursor ions was established and is presented in Table 3. This list is not exhaustive. First, since it was not possible to generalize the reactions with the $O_2^{\bullet +}$ precursor ion, it was not possible to predict specific product ions from this reaction. Second, some product ions may be missing; additional reaction mechanisms specific to the arylphosphate esters may exist that could not be highlighted solely with our experimental study of the alkylphosphate esters. However, this is a preliminary approach for the simple and rapid detection of TPP and TCP in air. It is important to note that even though the generation of these pure compounds presents some challenges, they can nevertheless be present in environmental phases, including air,[2,11] and their detection is a major issue that needs to be addressed in environmental analytical chemistry.

Reaction Kinetics. As specified previously, quantification by SIFT-MS requires the knowledge of the reaction rate constants *k* (Eq 1). A preliminary approach assumed that all collisions between the analytes and the precursor ions lead to an effective reaction, i.e., the constant *k* is equal to the collisional rate constant k_c.

The collisional rate constants k_c were calculated according to parametrized trajectory calculations using the dipole moment μ_r and the polarizability α of the neutral molecule and the reduced mass of the collisional ion-molecule partners. Table 4 summarizes the values of these constants for the six studied organophosphate esters.

For accurate quantification of compound concentrations at the ppb level with SIFT-MS, the reaction rate constants must be high, i.e., higher than 10^{-10} cm^3 s^{-1}. The collisional rate constants of all the studied compounds with the six reactive precursor ions (H_3O^+, NO^+, O_2^+, OH^-, $O^{\bullet -}$ and $O_2^{\bullet -}$) were high. It should be noted that the reaction rate constant *k* could be lower than the collision rate constant. Previously, in many similar studies, reaction rate constants *k* were determined for NO^+ and O_2^+ reactions, and these were sometimes lower than the collision rate constants k_c.[61] Similarly, the reactions of the anions could be slower. This assumption is correct for the proton transfer reactions with the hydronium ion. Since the collisional rate constant is inversely proportional to the reduced mass of the ion-molecule complex, its value was the highest with the $O^{\bullet -}$ precursor ion and lowest with the $O_2^{\bullet +}$ and $O_2^{\bullet -}$ precursors. Note that the collisional rate constants of the three TCP isomers were significantly different due to variations in their dipole moments and polarizabilities.

The quantification of the organophosphate esters by SIFT-MS is quite feasible according to the molecule's reactivities in the gas phase and their collisional constants. By assuming $k = k_c$ for the exothermic H_3O^+ proton transfer reactions, the limits of detection were determined and are detailed in Table 5. These values were quite low (from 7.9 to 39.8 µg m^{-3}), showing the relevance of the SIFT-MS measurements for semivolatile compounds such as organophosphate esters. In comparison with SPME-GC-MS techniques (Table 5), SIFT-MS technology is slightly less sensitive for the detection of organophosphate esters but has significant advantages, such as real-time measurements.

Table 3. Prediction of Product Ions from the Reaction of Triphenyl Phosphate (TPP) and Tricresyl Phosphate (TCP) with SIFT-MS Precursor Ions

Precursor ion	**Triphenyl phosphate $(C_6H_5O)_3PO$**	**Tricresyl phosphate $(C_7H_7O)_3PO$**
	Probable product ion (*m/z*)	Probable product ion (*m/z*)
H_3O^+	$(C_6H_5O)_3POH^+$ (327) $(C_6H_5O)_2P(OH)_2^+$ (251)	$(C_7H_7O)_3POH^+$ (369) $(C_7H_7O)_2P(OH)_2^+$ (279)
NO^+	$(C_6H_5O)_3PO.NO^+$ (356)	$(C_7H_7O)_3PO.NO^+$ (398)
OH^-	$(C_6H_5O)_2POO^-$ (249)	$(C_7H_7O)_2POO^-$ (277)
O^-	$(C_6H_5O)_2POO^-$ (249)	$(C_7H_7O)_2POO^-$ (277)

O_2^-	$(C_6H_5O)_2POO^-$ (249)	$(C_7H_7O)_2POO^-$ (277)

Table 4. Calculated Rate Constants kc for the Reactions of Organophosphate Esters with Precursor Ions in SIFT-MS

Compound	MW	α [a]	μ_r [a]	H_3O^+	NO^+	O_2^+	OH^-	$O^{\bullet-}$	$O_2^{\bullet-}$
				k_c [b]	k_c [b]	k_c [b]	k_c [b]	k_c [b]	k_c [b]
TEP	182	15.49	3.78	4.92	4.02	3.91	5.18	5.32	3.91
TBP	266	26.12	3.80	5.27	4.27	4.15	5.55	5.71	4.15
TCEP	284	20.55	2.49	3.85	3.12	3.03	4.06	4.18	3.03
TCPP	326	25.91	3.46	4.92	3.98	3.86	5.19	5.34	3.86
TPP	326	33.29	3.63	5.31	4.29	4.16	5.59	5.76	4.16
TpCP [c]	368	39.39	4.04	5.84	4.71	4.58	6.16	6.34	4.58
ToCP [d]	368	38.75	3.28	5.13	4.14	4.02	5.41	5.57	4.02
TmCP [e]	368	39.14	3.18	5.05	4.08	3.96	5.32	5.48	3.96

[a] α : polarizability (unit: 10^{-24} cm^3), μ_r : dipole moment (Debye); derived from DFT calculations.

[b] k_c: calculated collisional rate constants (units: 10^{-9} cm^3 s^{-1}).

[c] Tricresylphosphate with the methyl group in the para position.

[d] Tricresylphosphate with the methyl group in the ortho position.

[e] Tricresylphosphate with the methyl group in the meta position.

Table 5. Limits of Detection in SIFT-MS Using the H_3O^+ Precursor Ion Versus SPME-GC-MS Detection Limits (From a Previous Study[42])

Compound	Limits of detection (μg m^{-3})	
	SIFT-MS	SPME-GC-MS
TEP	7.9	2.5
TBP	20.2	1.2
TCEP	15.8	-
TCPP	38.6	1.1
TPP	29.0	-
TCP	39.8	-

Application: Investigation of Organophosphate Esters Emitted from Combustion-Modified High-Resilience Foams. Organophosphate esters are commonly used as flame retardants in polyurethane foams for upholstery. Generally, these additives are added during the polymerization process and are not chemically bound to the polymer. Consequently, they can migrate through the polymer material and be emitted into the air. Selected ion flow tube-mass spectrometry measurements were performed to study organophosphate ester emissions from combustion-modified high-resilience foams.

After a one-day incubation at 23°C, none of the six target compounds was detected in the headspace above the foams with any of the precursor ions. However, two organophosphate esters were detected in all the foam samples after incubation at 100°C: TBP and TCPP. The detection of each of the product ions listed above with the six reactive precursor ions (H_3O^+, NO^+, $O_2^{\bullet+}$, OH^-, $O^{\bullet-}$ and $O_2^{\bullet-}$) confirms the identification of these two compounds.

The quantification (with H_3O^+ precursor ions) of the emitted TBP and TCPP showed few differences between the four studied combustion-modified high-resilience foams: the TBP concentration emitted at 100°C varied from 32 to 80 mg $m^{-3,}$ and the TCPP concentrations ranged from 3.6 to 8.4 mg m^{-3} (Table 6). The concentrations emitted at 100°C were quite high (at the mg m^{-3} level) but consistent with previous reports.[4] The large difference between the emissions at 23°C and 100°C is consistent with the increase of vapor pressure with temperature. In fact, the temperature increase favors the emissions and decreases compound deposition onto the sampler surfaces. Considering these possible adsorption sink effects, the emissions measured at 23°C are probably underestimated.

From the measurements made at 100°C, it is possible to estimate the emissions at 23°C by extrapolation using the Clausius-Clapeyron law:[62]

$$ln\frac{P_1}{P_2} = \frac{\Delta Hv}{R}\left(\frac{1}{T_1} - \frac{1}{T_2}\right) \quad (12)$$

where P_1 and P_2 are the vapor pressures (Pa) at temperatures T_1 and T_2 (K), respectively, ΔHv is the enthalpy of vaporization (J mol^{-1}), and R is the ideal gas constant.

In the literature, some data are available for the enthalpies of vaporization of TBP or TCPP, addressing the phase changes from polyurethane foams to air or from pure liquid compounds to air.[63-65] This approach allows the estimation of emissions at a desired temperature (here, at 23°C). However, experimental measurements at a more elevated temperature limit the effect of the compound sink and strengthens the emission process. The values for the emission concentrations at 23°C obtained by this approach are reported in Table 6. As expected, the calculated concentrations were rather low (from 5 to 12 μg m^{-3}) for TCPP and were less than the instrumental detection limit (LOD = 38.6 μg m^{-3}, Table 5). For TBP, the estimated emission values at 23°C ranged from 57 to 144 μg m^{-3} and were higher than the LOD (20 μg m^{-3}), but the compound was not detected in the gas phase. This observation illustrates that adsorption to the glass bottle was a sink for TBP at 23°C.

These results are in agreement with measurements previously carried out for this type of material (polyurethane foams), with emissions on the order of a few mg m^{-3} for TBP and lower than 1 mg m^{-3} for TCPP.[42]

Table 6. Concentrations of Organophosphate Esters Detected in the Headspace after 24 h of Incubation of the Foams in a 1 L Bottle (Measurement by SIFT-MS with H_3O^+ Precursor ion) and Calculated by Extrapolation Using the Clausius-Clapeyron Law (With ΔHv = 80 kJ mol^{-1} for TBP and 81 kJ mol^{-1} for TCPP Given by,[61,62] Respectively)

Sample	Foam density (kg m^{-3})	TBP (µg m^{-3})			TCPP (µg m^{-3})		
		measured		calculated	measured		calculated
		23°C	100°C	23°C	23°C	100°C	23°C
Foam A	33	<LOD	3800	68.4	<LOD	840	11.8
Foam B	20	<LOD	5990	107.8	<LOD	360	5.1
Foam C	70	<LOD	3200	57.6	<LOD	810	11.4
Foam D	40	<LOD	8000	143.9	<LOD	370	5.2

CONCLUSIONS

This work is a first step toward the analysis of semivolatile organic compounds by SIFT-MS. Organophosphate esters reacted with six precursor ions, providing different possibilities for their analysis. The identified reaction schemes are in good agreement with literature reports for the SIFT-MS precursor ions and were confirmed by a computational approach. From these reaction schemes, predict ions and kinetic constants were also determined for TPP and TCT, even if these compounds were not be generated in air during this work. Thus, the protonation of organophosphate esters upon reacting with H_3O^+ is not surprising. Similarly, the S_N2 nucleophilic substitution reaction of the chlorinated esters with OH^-, $O^{\bullet-}$ and $O_2^{\bullet-}$, which are good nucleophiles in the gas phase, were also expected.

The collision rate constants were high enough for the quantification of all six target compounds with the six reactive precursor ions. Thus, it was possible to not only detect but also quantify the organophosphates in the gas phase, as in the presented example of the analysis of emissions from combustion-modified high-resilience foams.

The quantification method using the collision rate constant k_c is a preliminary approach. This approximation, often encountered in the literature for SIFT-MS measurements with H_3O^+ precursor ions when the proton transfer reaction is exothermic, is feasible for measurements of organophosphate esters. Although this approach is valid for hydronium ions, it has yet to be verified for the other precursor ions. Studies on other compounds tend to show that the reaction rate constant k can be lower than the collision rate constant k_c, especially for the NO^+ and O_2^+ ions. The quantification process could be refined by experimental determination of the reaction rate constants k. However, this approach requires the generation of standard atmospheres with controlled concentrations, which is currently a considerable barrier to the analysis of semivolatile organic compounds. Although this preliminary approach can be improved, it allows for the classification of materials according to their emissions.

Because of its speed and ease of use, selected ion flow tube – mass spectrometry is highly relevant for the rapid screening and classification of compounds emitted from materials and offers new perspectives for the analysis of semivolatile organic compounds in air, such as organophosphate esters. The high-frequency analysis rate of SIFT-MS measurements allows the detection and quantification of these OPEs in air in real time. This application offers interesting perspectives for monitoring indoor air quality, especially for short emission events such as aircraft cabin emissions during flight.

AUTHOR INFORMATION

*Corresponding Author

Mickael Le Bechec
Universite de Pau et des Pays de l'Adour, E2S UPPA, CNRS, IPREM, Institut des sciences analytiques et de Physicochimie pour l'environnement et les Matériaux, UMR5254, Hélioparc, 2 avenue Président Angot, 64053, PAU cedex 9, France
e-mail: mickael.lebechec@univ-pau.fr

Author Contributions

MG and MLB designed the study and wrote the manuscript, MG, MR and HP performed the experiments and analyzed the data, JMS performed the computational experiments, TP funded the instrument and MLB reviewed, edited the manuscript and supervised the project.

Notes

The authors declare no competing financial interest.

ACKNOWLEDGMENT

REFERENCES

(1) Stapleton, H. M.; Sharma, S.; Getzinger, G.; Ferguson, P. L.; Gabriel, M.; Webster, T. F.; Blum, A. Novel and High Volume Use Flame Retardants in US Couches Reflective of the 2005 PentaBDE Phase Out. *Environ. Sci. Technol.* **2012**, *46* (24), 13432–13439. DOI: 10.1021/es303471d

(2) Van der Veen, I.; De Boer, J. Phosphorus Flame Retardants: Properties, Production, Environmental Occurrence, Toxicity and Analysis. *Chemosphere* **2012**, *88* (10), 1119–1153. DOI: 10.1016/j.chemosphere.2012.03.067

(3) Stapleton, H. M.; Klosterhaus, S.; Eagle, S.; Fuh, J.; Meeker, J. D.; Blum, A.; Webster, T. F. Detection of Organophosphate Flame Retardants in Furniture Foam and U.S. House Dust. *Environ. Sci. Technol.* **2009**, *43* (19), 7490–7495. DOI: 10.1021/es9014019

(4) Ghislain, M.; Beigbeder, J.; Dumazert, L.; Lopez-Cuesta, J. M.; Lounis, M.; Leconte, S.; Desauziers, V. Determination of the Volatile Fraction of Phosphorus Flame Retardants in Cushioning Foam of Upholstered Furniture: Towards Respiratory Exposure Assessment. *Environ. Monit. Assess.* **2016**, *188* (10), 576. DOI: 10.1007/s10661-016-5566-y

(5) Mendelsohn, E.; Hagopian, A.; Hoffman, K.; Butt, C. M.; Lorenzo, A.; Congleton, J.; Webster, T. F.; Stapleton, H. M. Nail

Polish as a Source of Exposure to Triphenyl Phosphate. *Environ. Int.* **2016**, *86*, 45–51. DOI: 10.1016/j.envint.2015.10.005

(6) Hoffman, K.; Butt, C. M.; Chen, A.; Limkakeng, A. T., Jr.; Stapleton, H. M. High Exposure to Organophosphate Flame Retardants in Infants: Associations with Baby Products. *Environ. Sci. Technol.* **2015**, *49* (24), 14554–14559. DOI: 10.1021/acs.est.5b03577

(7) Marklund, A.; Andersson, B.; Haglund, P. Screening of Organophosphorus Compounds and Their Distribution in Various Indoor Environments. *Chemosphere* **2003**, *53* (9), 1137–1146. DOI: 10.1016/s0045-6535(03)00666-0

(8) Megson, D.; Ortiz, X.; Jobst, K. J.; Reiner, E. J.; Mulder, M. F.; Balouet, J. C. A Comparison of Fresh and Used Aircraft Oil for the Identification of Toxic Substances Linked to Aerotoxic Syndrome. *Chemosphere* **2016**, *158*, 116–123. DOI: 10.1016/j.chemosphere.2016.05.062

(9) Wei, G. L.; Li, D. Q.; Zhuo, M. N.; Liao, Y. S.; Xie, Z. Y.; Guo, T. L.; Li, J. J.; Zhang, S. Y.; Liang, Z. Q. Organophosphorus Flame Retardants and Plasticizers: Sources, Occurrence, Toxicity and Human Exposure. *Environ. Pollut.* **2015**, *196*, 29–46. DOI: 10.1016/j.envpol.2014.09.012

(10) He, R.; Li, Y.; Xiang, P.; Li, C.; Zhou, C.; Zhang, S.; Cui, X.; Ma, L. Q. Organophosphorus Flame Retardants and Phthalate Esters in Indoor Dust from Different Microenvironments: Bioaccessibility and Risk Assessment. *Chemosphere* **2016**, *150*, 528–535. DOI: 10.1016/j.chemosphere.2015.10.087

(11) Hou, M.; Shi, Y.; Na, G.; Cai, Y. A Review of Organophosphate Esters in Indoor Dust, Air, Hand Wipes and Silicone Wristbands: Implications for Human Exposure. *Environ. Int.* **2021**, *146*, 106261. DOI: 10.1016/j.envint.2020.106261

(12) Fan, Q.; Zou, X.; Gao, J.; Cheng, Y.; Wang, C.; Feng, Z.; Ding, Y.; Zhang, C. Assessing Ecological Risk of Organophosphate Esters Released from Sediment with Both of Total Content and Desorbable Content. *Sci. Total Environ.* **2021**, *772*, 144907. DOI: 10.1016/j.scitotenv.2020.144907

(13) Picó, Y.; Campo, J.; Alfarhan, A. H.; El-Sheikh, M. A.; Barceló, D. A Reconnaissance Study of Pharmaceuticals, Pesticides, Perfluoroalkyl Substances and Organophosphorus Flame Retardants in the Aquatic Environment, Wild Plants and Vegetables of Two Saudi Arabia Urban Areas: Environmental and Human Health Risk Assessment. *Sci. Total Environ.* **2021**, *776*, 145843. DOI: 10.1016/j.scitotenv.2021.145843

(14) Reemtsma, T.; Quintana, J. B.; Rodil, R.; Garcı´a-López, M.; Rodrı´guez, I. Organophosphorus Flame Retardants and Plasticizers in Water and Air I. Occurrence and Fate. *TrAC Trends Anal. Chem.* **2008**, *27* (9), 727–737. DOI: 10.1016/j.trac.2008.07.002

(15) Greaves, A. K.; Letcher, R. J. A Review of Organophosphate Esters in the Environment from Biological Effects to Distribution and Fate. *Bull. Environ. Contam. Toxicol.* **2017**, *98* (1), 2–7. DOI: 10.1007/s00128-016-1898-0

(16) Hayes, K.; Megson, D.; Doyle, A.; O'Sullivan, G. Occupational Risk of Organophosphates and Other Chemical and Radiative Exposure in the Aircraft Cabin: A Systematic Review. *Sci. Total Environ.* **2021**, *796*, 148742. DOI: 10.1016/j.scitotenv.2021.148742

(17) Schreder, E. D.; Uding, N.; La Guardia, M. J. Inhalation a Significant Exposure Route for Chlorinated Organophosphate Flame Retardants. *Chemosphere* **2016**, *150*, 499–504. DOI: 10.1016/j.chemosphere.2015.11.084

(18) Hou, R.; Xu, Y.; Wang, Z. Review of OPFRs in Animals and Humans: Absorption, Bioaccumulation, Metabolism, and Internal Exposure Research. *Chemosphere* **2016**, *153*, 78–90. DOI: 10.1016/j.chemosphere.2016.03.003

(19) Li, J.; Zhao, L.; Letcher, R. J.; Zhang, Y.; Jian, K.; Zhang, J.; Su, G. A Review on Organophosphate Ester (OPE) Flame Retardants and Plasticizers in Foodstuffs: Levels, Distribution, Human Dietary Exposure, and Future Directions. *Environ. Int.* **2019**, *127*, 35–51. DOI: 10.1016/j.envint.2019.03.009

(20) Ding, J.; Deng, T.; Xu, M.; Wang, S.; Yang, F. Residuals of Organophosphate Esters in Foodstuffs and Implication for Human Exposure. *Environ. Pollut.* **2018**, *233*, 986–991. DOI: 10.1016/j.envpol.2017.09.092

(21) Gbadamosi, M. R.; Abdallah, M. A.; Harrad, S. A Critical Review of Human Exposure to Organophosphate Esters with a Focus on Dietary Intake. *Sci. Total Environ.* **2021**, *771*, 144752. DOI: 10.1016/j.scitotenv.2020.144752

(22) Phillips, A. L.; Hammel, S. C.; Hoffman, K.; Lorenzo, A. M.; Chen, A.; Webster, T. F.; Stapleton, H. M. Children's Residential Exposure to Organophosphate Ester Flame Retardants and Plasticizers: Investigating Exposure Pathways in the TESIE Study. *Environ. Int.* **2018**, *116*, 176–185. DOI: 10.1016/j.envint.2018.04.013

(23) Liu, X.; Yu, G.; Cao, Z.; Wang, B.; Huang, J.; Deng, S.; Wang, Y. Occurrence of Organophosphorus Flame Retardants on Skin Wipes: Insight into Human Exposure from Dermal Absorption. *Environ. Int.* **2017**, *98*, 113–119. DOI: 10.1016/j.envint.2016.10.021

(24) Castorina, R.; Butt, C.; Stapleton, H. M.; Avery, D.; Harley, K. G.; Holland, N.; Eskenazi, B.; Bradman, A. Flame Retardants and Their Metabolites in the Homes and Urine of Pregnant Women Residing in California (the CHAMACOS Cohort). *Chemosphere* **2017**, *179*, 159–166. DOI: 10.1016/j.chemosphere.2017.03.076

(25) Meeker, J. D.; Cooper, E. M.; Stapleton, H. M.; Hauser, R. Urinary Metabolites of Organophosphate Flame Retardants: Temporal Variability and Correlations with House Dust Concentrations. *Environ. Health Perspect.* **2013**, *121* (5), 580–585. DOI: 10.1289/ehp.1205907

(26) Cequier, E.; Sakhi, A. K.; Marcé, R. M.; Becher, G.; Thomsen, C. Human Exposure Pathways to Organophosphate Triesters - A Biomonitoring Study of Mother-Child Pairs. *Environ. Int.* **2015**, *75*, 159–165. DOI: 10.1016/j.envint.2014.11.009

(27) Hammel, S. C.; Zhang, S.; Lorenzo, A. M.; Eichner, B.; Stapleton, H. M.; Hoffman, K. Young Infants' Exposure to Organophosphate Esters: Breast Milk as a Potential Source of Exposure. *Environ. Int.* **2020**, *143*, 106009. DOI: 10.1016/j.envint.2020.106009

(28) Doherty, B. T.; Hammel, S. C.; Daniels, J. L.; Stapleton, H. M.; Hoffman, K. Organophosphate Esters: Are These Flame Retardants and Plasticizers Affecting Children's Health? *Curr. Environ. Health Rep.* **2019**, *6* (4), 201–213. DOI: 10.1007/s40572-019-00258-0

(29) Araki, A.; Saito, I.; Kanazawa, A.; Morimoto, K.; Nakayama, K.; Shibata, E.; Tanaka, M.; Takigawa, T.; Yoshimura, T.; Chikara, H.; Saijo, Y.; Kishi, R. Phosphorus Flame Retardants in Indoor Dust and Their Relation to Asthma and Allergies of Inhabitants. *Indoor Air* **2014**, *24* (1), 3–15. DOI: 10.1111/ina.12054

(30) Liu, Y.; Li, Y.; Dong, S.; Han, L.; Guo, R.; Fu, Y.; Zhang, S.; Chen, J. The Risk and Impact of Organophosphate Esters on the Development of Female-Specific Cancers: Comparative Analysis of Patients with Benign and Malignant Tumors. Journal of Hazardous Materials 2021, 404, 124020. https://doi.org/10.1016/j.jhazmat.2020.124020.

(31) Li, Y.; Fu, Y.; Hu, K.; Zhang, Y.; Chen, J.; Zhang, S.; Zhang, B.; Liu, Y. Positive Correlation between Human Exposure to Organophosphate Esters and Gastrointestinal Cancer in Patients from Wuhan, China. Ecotoxicology and Environmental Safety 2020, 196, 110548. https://doi.org/10.1016/j.ecoenv.2020.110548.

(32) Barrett, D. S.; Oehme, F. W. The Effect of a Single Oral Dose of Tri-O-Cresyl Phosphate on Neurotoxic Esterase and Acetylcholinesterase Activities in the Central Nervous System, Erythrocytes and Plasma. Veterinary and Human Toxicology 1994, 36 (1), 1–4.

(33) Duarte, D. J.; Rutten, J. M. M.; van den Berg, M.; Westerink, R. H. S. In Vitro Neurotoxic Hazard Characterization of Different Tricresyl Phosphate (TCP) Isomers and Mixtures. NeuroToxicology 2017, 59, 222–230. https://doi.org/10.1016/j.neuro.2016.02.001.

(34) Liu, X.; Ji, K.; Choi, K. Endocrine Disruption Potentials of Organophosphate Flame Retardants and Related Mechanisms in H295R and MVLN Cell Lines and in Zebrafish. Aquatic Toxicology 2012, 114–115, 173–181. https://doi.org/10.1016/ j.aquatox. 2012.02.019.

(35) Schang, G.; Robaire, B.; Hales, B. F. Organophosphate Flame Retardants Act as Endocrine-Disrupting Chemicals in MA-10 Mouse Tumor Leydig Cells. Toxicol. Sci. 2016, 150 (2), 499–509. https://doi.org/10.1093/toxsci/kfw012.

(36) Zhang, Q.; Lu, M.; Dong, X.; Wang, C.; Zhang, C.; Liu, W.; Zhao, M. Potential Estrogenic Effects of Phosphorus-Containing Flame Retardants. *Environ. Sci. Technol.* **2014**, *48* (12), 6995–7001. DOI: 10.1021/es5007862

(37) Zhang, Q.; Ji, C.; Yin, X.; Yan, L.; Lu, M.; Zhao, M. Thyroid Hormone-Disrupting Activity and Ecological Risk Assessment of Phosphorus-Containing Flame Retardants by In Vitro, In Vivo and in Silico Approaches. *Environ. Pollut.* **2016**, *210*, 27–33. DOI: 10.1016/j.envpol.2015.11.051

(38) He, C.; Wang, X.; Thai, P.; Baduel, C.; Gallen, C.; Banks, A.; Bainton, P.; English, K.; Mueller, J. F. Organophosphate and Brominated Flame Retardants in Australian Indoor Environments: Levels, Sources, and Preliminary Assessment of Human Exposure. *Environ. Pollut.* **2018**, *235*, 670–679. DOI: 10.1016/j.envpol.2017.12.017

(39) Vykoukalová, M.; Venier, M.; Vojta, Š.; Melymuk, L.; Bečanová, J.; Romanak, K.; Prokeš, R.; Okeme, J. O.; Saini, A.; Diamond, M. L.; Klánová, J. Organophosphate Esters Flame Retardants in the Indoor Environment. *Environ. Int.* **2017**, *106*, 97–104. DOI: 10.1016/j.envint.2017.05.020

(40) Bergh, C.; Magnus Åberg, K.; Svartengren, M.; Emenius, G.; Östman, C. Organophosphate and Phthalate Esters in Indoor Air: A Comparison between Multi-Storey Buildings with High and Low Prevalence of Sick Building Symptoms. *J. Environ. Monit.* **2011**, *13* (7), 2001–2009. DOI: 10.1039/c1em10152h

(41) Tao, F.; Sellström, U.; De Wit, C. A. Organohalogenated Flame Retardants and Organophosphate Esters in Office Air and Dust from Sweden. *Environ. Sci. Technol.* **2019**, *53* (4), 2124–2133. DOI: 10.1021/acs.est.8b05269

(42) Ghislain, M.; Beigbeder, J.; Plaisance, H.; Desauziers, V. New Sampling Device for On-Site Measurement of SVOC Gas-Phase Concentration at the Emitting Material Surface. *Anal. Bioanal. Chem.* **2017**, *409* (12), 3199–3210. DOI: 10.1007/s00216-017-0259-0

(43) Plaisance, H.; Ghislain, M.; Desauziers, V. Assessment of Gas-Phase Concentrations of Organophosphate Flame Retardants at the Material Surface Using a Midget Emission Cell Coupled to Solid-Phase Microextraction. *Anal. Chim. Acta* **2021**, *1186*, 339100. DOI: 10.1016/j.aca.2021.339100

(44) Salthammer, T.; Bahadir, M. Occurrence, Dynamics and Reactions of Organic Pollutants in the Indoor Environment. *CLEAN Soil Air Water* **2009**, *37* (6), 417–435. DOI: 10.1002/clen.200900015

(45) Smith, D.; Spanel, P. Selected Ion Flow Tube Mass Spectrometry (SIFT-MS) for On-Line Trace Gas Analysis. *Mass Spectrom. Rev.* **2005**, *24* (5), 661–700. DOI: 10.1002/mas.20033

(46) Smith, D.; Cheng, P.; Spanel, P. Analysis of Petrol and Diesel Vapour and Vehicle Engine Exhaust Gases Using Selected Ion Flow Tube Mass Spectrometry. *Rapid Commun. Mass Spectrom.* **2002**, *16* (11), 1124–1134. DOI: 10.1002/rcm.691

(47) Francis, G. J.; Wilson, P. F.; Milligan, D. B.; Langford, V. S.; McEwan, M. J. GeoVOC: A SIFT-MS Method for the Analysis of Small Linear Hydrocarbons of Relevance to Oil Exploration. *Int. J. Mass Spectrom.* **2007**, *268* (1), 38–46. DOI: 10.1016/j.ijms.2007.08.005

(48) Spanel, P.; Smith, D. On the Features, Successes and Challenges of Selected Ion Flow Tube Mass Spectrometry. *Eur. J. Mass Spectrom.* **2013**, *19* (4), 225–246. DOI: 10.1255/ejms.1240

(49) Dhooghe, F.; Amelynck, C.; Schoon, N.; Debie, E.; Bultinck, P.; Vanhaecke, F. A Selected Ion Flow Tube Study of the Reactions of H3O+, NO+ and O2+ with a Series of Sesquiterpenes. *Int. J. Mass Spectrom.* **2008**, *272* (2-3), 137–148. DOI: 10.1016/j.ijms.2008.02.002

(50) Hera, D.; Langford, V. S.; McEwan, M. J.; McKellar, T. I.; Milligan, D. B. Negative Reagent Ions for Real Time Detection Using SIFT-MS. *Environments* **2017**, *4* (1), 16. DOI: 10.3390/environments4010016

(51) Francis, G. J.; Milligan, D. B.; McEwan, M. J. Detection and Quantification of Chemical Warfare Agent Precursors and Surrogates by Selected Ion Flow Tube Mass Spectrometry. *Anal. Chem.* **2009**, *81* (21), 8892–8899. DOI: 10.1021/ac901486c

(52) Smith, D.; McEwan, M. J.; Španěl, P. Understanding Gas Phase Ion Chemistry is the Key to Reliable Selected Ion Flow Tube-Mass Spectrometry Analyses. *Anal. Chem.* **2020**, *92* (19), 12750–12762. DOI: 10.1021/acs.analchem.0c03050

(53) Ghislain, M.; Costarramone, N.; Sotiropoulos, J. M.; Pigot, T.; Van den Berg, R.; Lacombe, S.; Le Bechec, M. Direct Analysis of Aldehydes and Carboxylic Acids in the Gas Phase by Negative Ionization Selected Ion Flow Tube Mass Spectrometry: Quantification and Modelling of Ion-Molecule Reactions. *Rapid Commun. Mass Spectrom.* **2020**, *33* (21), 1623–1634. DOI: 10.1002/rcm.8504

(54) Ghislain, M.; Costarramone, N.; Pigot, T.; Reyrolle, M.; Lacombe, S.; Le Bechec, M. High Frequency Air Monitoring by Selected Ion Flow Tube-Mass Spectrometry (SIFT-MS): Influence of the Matrix for Simultaneous Analysis of VOCs, CO_2, Ozone and Water. *Microchem. J.* **2020**, *153*, 104435. DOI: 10.1016/j.microc.2019.104435

(55) Ghislain, M.; Reyrolle, M.; Sotiropoulos, J. M.; Pigot, T.; Le Bechec, M. Chemical Ionization of Carboxylic Acids and Esters in Negative Mode Selected Ion Flow Tube – Mass Spectrometry (SIFT-MS). *Microchem. J.* **2021**, *169*, 106609. DOI: 10.1016/j.microc.2021.106609

(56) Gaussian. 16, Revision C.01, Frisch, M. J; Published Online 2019. **2019**.

(57) Su, T.; Chesnavich, W. J. Parametrization of the Ion–Polar Molecule Collision Rate Constant by Trajectory Calculations. *J. Chem. Phys.* **1982**, *76* (10), 5183–5185. DOI: 10.1063/1.442828

(58) Bohme, D. The Kinetics and Energetics of Proton Transfer. In *Interactions between Ions and Molecules*; Ausloos, P. Ed.; New York, NY, (1975); pp 489–504.

(59) Španěl, P.; Pavlik, M.; Smith, D. Reactions of H3O+ and OH− Ions with Some Organic Molecules; Applications to Trace Gas Analysis in Air. *Int. J. Mass Spectrom. Ion Processes* **1995**, *145* (3), 177–186. DOI: 10.1016/0168-1176(95)04164-G

(60) Spanel, P.; Smith, D. SIFT Studies of the Reactions of H3O+, NO+ and O2+ with a Series of Alcohols. *Int. J. Mass Spectrom. Ion Processes* **1997**, *167-168*, 375–388. DOI: 10.1016/S0168-1176(97)00085-2

(61) Smith, D.; Wang, T.; Španěl, P. A SIFT Study of the Reactions of H2ONO+ Ions with Several Types of Organic Molecules. *Int. J. Mass Spectrom.* **2003**, *230* (1), 1–9. DOI: 10.1016/S1387-3806(03)00341-5

(62) Cao, J.; Zhang, X.; Little, J. C.; Zhang, Y. A SPME-Based Method for Rapidly and Accurately Measuring the Characteristic Parameter for DEHP Emitted from PVC Floorings. *Indoor Air* **2017**, *27* (2), 417–426. DOI: 10.1111/ina.12312

(63) Tian, S.; Sebroski, J.; Ecoff, S. Predicting TCPP Emissions and Airborne Concentrations from Spray Polyurethane Foam Using USEPA I-SVOC Software: Parameter Estimation and Result Interpretation. In *Developing Consensus Standards for Measuring Chemical Emissions from Spray Polyurethane Foam (SPF) Insulation*; Sebroski, J., Mason, M. Eds.; ASTM International, (2017); pp 167–198.

(64) Panneerselvam, K.; Antony, M.; Srinivasan, T.; Rao, P. V. Measurement of Enthalpies of Vaporization of Trialkyl Phosphates Using Correlation Gas Chromatography. *Thermochim. Acta* **2007**, *466* (1-2), 49–56. DOI: 10.1016/j.tca.2007.10.007

(65) Srirachat, W.; Pancharoen, U.; Kheawhom, S. An Investigation of Saturated Vapor Pressure Regarding Low-Volatility Organophosphorus Extractants Di-(2-ethylhexyl) Phosphoric Acid and Tributyl Phosphate: Correlation and Thermodynamics Study. *Vacuum* **2018**, *156*, 237–247. DOI: 10.1016/j.vacuum.2018.07.036

TABLE OF CONTENTS GRAPHIC